



Use of infrared thermography to investigate the fatigue behavior of a carbon fiber reinforced polymer composite

John Montesano^{a,*}, Zouheir Fawaz^a, Habiba Bougherara^b

^a Dept. of Aerospace Eng., Ryerson University, 350 Victoria St., Toronto, Canada M5B 2K3

^b Dept. of Mechanical and Industrial Eng., Ryerson University, 350 Victoria St., Toronto, Canada M5B 2K3

ARTICLE INFO

Article history:

Available online 6 November 2012

Keywords:

Polymer matrix composite materials
Fatigue
Thermography
Material properties

ABSTRACT

Thermography was used to investigate the fatigue behavior of a braided carbon fiber polymeric composite plate. A thermographic approach, originally developed in an earlier study for metallic alloys, was employed to rapidly determine the composite high cycle fatigue strength. The method yielded a fatigue threshold value that was in excellent agreement with that obtained through a conventional experimental test program. The damage mechanisms responsible for the increased heat dissipation and ultimately failure were identified, which provides support for the existence of a fatigue threshold for this material. An extension of the thermographic technique to rapidly determine the entire fatigue stress-life curve for the composite plate provided a direct correlation to the stress-life curve determined through a conventional test program. Energy dissipation was also used as an indicator to determine the high cycle fatigue strength, providing support for the thermographic approach. A relationship between the dissipated heat, the intrinsic energy dissipation and the number of cycles to failure has been clearly established.

© 2012 Elsevier Ltd. All rights reserved.

1. Introduction

In recent years, advanced polymer matrix composite (PMC) materials have been more frequently employed for manufacturing aerospace, automotive and marine load-bearing components due to their lightweight and high strength. Specifically, the development of two-dimensional and three-dimensional braided PMC materials has excelled due to a number of clear advantages including superior fatigue performance and lower manufacturing costs [1,2]. In spite of the indicated advantages, the use of braided PMC materials is however limited to few practical applications. One of the issues limiting their widespread use is that few studies have been conducted which restricts the available mechanical performance data of these materials [3–8]. Damage and failure mechanisms are more complex for braided PMCs and thus much more difficult to understand, partially due to a number of fabric geometric variables such as tow size, tow angle and braid pattern. Generally, there is a lack in available fatigue life and fatigue strength data for braided materials, which would otherwise be useful during the component design stage or for operational maintenance planning. Fatigue degradation caused by cyclic loading is a common mode of failure for in-service components.

In order to provide practical information on the fatigue behavior and the damage state of materials, a number of well established non-destructive methods have been employed [9–11]. These

methods may not necessarily be practical for in situ monitoring due mainly to the limitations of the testing apparatus. The use of infrared thermography (IRT) for in situ detection of fatigue damage in materials has recently been established as a valid non-destructive evaluation (NDE) technique [12,13]. Specifically, the thermographic approach for rapidly determining the fatigue strength of metals, as originally developed by Risitano and co-workers [14], has been well documented in the literature [15,16]. The application of this method has also shown to be useful for the determination of the high cycle fatigue strength (HCFS) of some composite materials [17–19]. The main advantage of using this approach is that few test components and only a few hours are required to determine the HCFS with sufficient accuracy. It is therefore the objective of this study to employ and validate the thermographic approach for rapidly determining the HCFS of a triaxially braided fiber-reinforced PMC plate. To the knowledge of the authors, this is a novel application for the aforementioned thermographic technique. In addition, the calculated energy dissipation from the experimental stress-strain fatigue data will also be used to determine the HCFS and will be compared with the thermographic results for validation of that technique. Finally, the entire stress-life ($S-N$) curve for the material will be developed using the thermographic approach, which is also a novel result for fiber-reinforced PMC materials.

2. IRT background

As indicated, IRT is a well established non-contact NDE technique for monitoring fatigue damage in structural components.

* Corresponding author. Tel.: +1 416 979 5000x4887; fax: +1 416 979 5056.
E-mail address: gmontesa@ryerson.ca (J. Montesano).

Thermography is a measurement technique that relies on the use of an infrared (IR) camera to provide a time-dependent contour map of an objects surface temperature. This technique involves decoding temperature information which results from the IR radiation emitted by an object. This can be done actively via external heating or using a passive heating approach [12]. The passive approach is ideal for cyclic loading because the resulting hysteretic heating allows for a time-dependent temperature variation which can be monitored with the IR camera. The recorded images can then be analyzed to determine the material fatigue strength or to understand damage initiation and development. Analyzing the images can however be a challenge since the detected temperature rise may be due to a number of different phenomena.

From an irreversible thermodynamics framework, the temperature T , strain tensor $\boldsymbol{\varepsilon}$ and internal variable vector $\boldsymbol{\alpha} = \alpha_i$ can describe the thermodynamic state of any continuous solid. The Clausius–Duhem inequality based on the second law of thermodynamics can be used to describe the dissipation (d) due to various irreversible phenomena, and can be expressed as:

$$d = \boldsymbol{\sigma} : \mathbf{D} - \rho \psi_{,e} : \dot{\boldsymbol{\varepsilon}} - \rho \psi_{,\alpha} \cdot \dot{\boldsymbol{\alpha}} - \frac{\mathbf{q}}{T} \cdot \text{grad}T \geq 0 \quad (1)$$

where $\boldsymbol{\sigma}$ is the Cauchy stress tensor, \mathbf{D} is the strain rate tensor, ρ is the scalar mass density, ψ is the specific free energy function and \mathbf{q} is the heat influx vector. The dot represents a material time derivative. This leads to the local heat conduction equation defined as [20]:

$$\rho C_{e,\alpha} \dot{T} + \text{div} \mathbf{q} = r + \rho T \psi_{,T,e} : \dot{\boldsymbol{\varepsilon}} + \rho T \psi_{,T,\alpha} \cdot \dot{\boldsymbol{\alpha}} + d_{\text{int}} \quad (2)$$

where $C_{e,\alpha}$ denotes specific heat capacity, d_{int} the intrinsic dissipation (or local entropy production) and r the heat source. The local heat conduction equation includes heat dissipation caused by heat sources (r), thermo-mechanical coupling terms ($\rho T \psi_{,T,e} : \dot{\boldsymbol{\varepsilon}}$, $\rho T \psi_{,T,\alpha} \cdot \dot{\boldsymbol{\alpha}}$) and intrinsic dissipation (d_{int}). For the employment of a passive heating thermographic technique, considering Eq. (2) is key for using temperature as an indicator of damage and to allow for proper interpretation of the acquired thermal images. It has been shown that the intrinsic energy dissipation (d_{int}) of metallic materials is the main contributor to heat dissipation, and thus the most accurate indicator of damage manifestation [15]. Therefore, tracking the temperature increase in composite materials during cyclic loading may also be the most accurate method to monitor intrinsic energy dissipation. Consequently by this reasoning, hysteretic heating would effectively be a measure of the energy dissipated (or energy absorbed) by the material due to internal irreversible phenomena.

3. Thermographic approach details

In order to effectively use this thermographic approach to determine the fatigue limit of a metallic alloy or the HCFS of a PMC material, it is necessary to understand the mechanisms that would cause intrinsic energy dissipation and thus heat dissipation. For ductile metallic alloys, fatigue failure can occur at stress levels that are significantly lower than the yield strength. On the microscopic scale metals are neither isotropic nor homogeneous and can therefore exhibit local fluctuations in stress, which can exceed the material yield limit causing plastic strains even though the macroscopic stress causes elastic strain. When subjected to repeated loading microscopic phenomena can therefore initiate and develop under these elastic stresses, causing heat to emanate from the material [15]. These local phenomena may include persistent slip bands along primary slip planes (i.e., local plasticity) and microscopic cracking at the grain boundaries (i.e., microscopic damage). These are two potential causes of intrinsic energy dissipation (d_{int})

in ductile metallic alloys subjected to cyclic loading. In PMC materials subjected to macroscopically applied elastic stresses, similar local microscopic stress fluctuations can cause intrinsic energy dissipation. The main mechanisms causing energy dissipation may be attributed to the viscoelastic nature of the matrix material, matrix cracking, fiber fracture, and interface cracking/friction among others [12]. Specifically for a textile composite, additional dissipative mechanisms may include matrix deformation and fiber reorientation for off-axis loading conditions [21]. It has been documented that these mechanisms are not prevalent when metals are stressed below their fatigue limit, but become more prevalent when the fatigue limit is exceeded [14]. This allows for the potential use of the thermographic approach to determine the HCFS of composites.

The thermographic approach for determining the fatigue limit of various metallic alloys has been successfully employed in numerous studies, with some variations on the application of the method. Luong [15] and LaRosa and Risitano [14] monitored the energy dissipated at various stress levels by measuring the temperature difference between two states of various metallic alloys. In the former study, the temperature of a steel specimen was compared before and after the application of several thousand loading cycles. The difference in temperature was a rising function of the applied stress amplitude, which was initially slow and then suddenly accelerated. The fatigue limit was found from this thermo-mechanical threshold. In the latter study, various steel specimens were cycled resulting in a temperature rise up to a plateau whose magnitude depends on the stress magnitude. The fatigue limit was found by plotting the temperature parameter as a function of the applied stress amplitude and interpolating to zero temperature level. In addition to monitoring the dissipated energy, Krapez and Pacou [16] also monitored the two Fourier components that are based on the cyclic loading frequency using a lock-in thermography approach for aluminum alloys. It was shown that by monitoring these two parameters, the fatigue limit of alloy steels and aluminum could also be found. Bremond [22] employed a similar approach using the lock-in D-mode option with a Cedip IR camera for determining the fatigue limit of an aluminum alloy. Quaresimin [17] used a form of Risitano's method for determining the HCFS of woven PMC laminates. A similar approach will be employed in this study on the aforementioned braided PMC plate.

The main points for proper application of Risitano's method will now be summarized. The method assumes that the recorded temperature variation caused by cyclic loading of a test specimen is a measure of the heat dissipation due to intrinsic energy dissipative mechanisms. The test specimen is cycled for a limited number of cycles at a given maximum stress level in order to produce stabilization of the surface temperature. This is repeated for many stress levels at a constant loading frequency, where the schematic of temperature variation vs. cycles for various stress levels is shown in Fig. 1a. For each stress level, the corresponding temperature increase from initial to stabilization can be plotted as a function of the applied stress as shown schematically in Fig. 1b. Then, from the plot it can be seen that when the threshold point is reached the temperature increase is greater and the fatigue limit can be determined. The hypothesis is that when the fatigue limit is exceeded, the heat dissipation drastically increases because of the increase in the degree of intrinsic energy dissipation.

4. Material and experimental details

The tested composite plate consists of a triaxially braided carbon fiber (T650/35–6 K) fabric, with a $0^\circ/\pm\theta$ braid orientation, embedded in a thermosetting polyimide resin. The flat composite panels were manufactured using a resin transfer molding (RTM) technique, and had final dimensions of 362 mm (warp) by

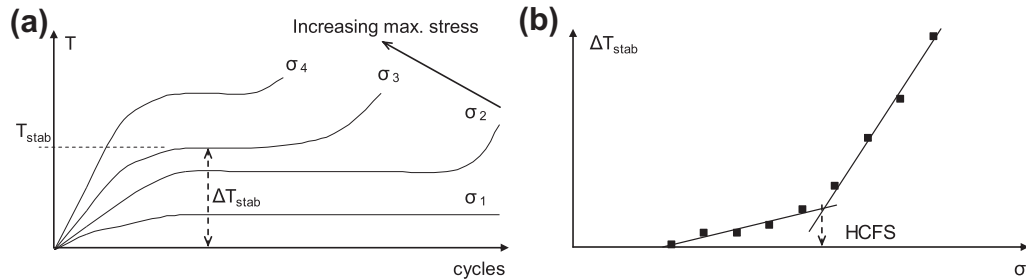


Fig. 1. Schematic of thermographic methodology for determining HCFS: (a) temperature-cycle profile, (b) temperature rise-stress profile.

350 mm. All panels were inspected for manufacturing defects using a thru-transmission immersion ultrasonic c-scan method; for all the panels, no visible defects were found. Each panel was cut along the warp direction (i.e., 0° yarn direction) into 12 specimens using an abrasive waterjet cutting technique. The nominal dimensions of each specimen were 355 mm \times 25 mm. The edges of all cut specimens were subsequently wet sanded with 180-grit and then 320-grit paper for improved edge quality. All test specimens were equipped with 10° tapered end tabs to eliminate any potential issues with gripping induced failure. The end tabs were manufactured from 3 mm thick by 25 mm wide 6061-T6 aluminum, and were bonded to the specimens using Loctite 496 adhesive.

In this study, the thermographic approach to determine the HCFS of the aforementioned material was employed and compared to the traditional approach which required a comprehensive experimental program aimed at constructing an $S-N$ curve. All uniaxial tensile tests were conducted at room temperature on an MTS 322 test frame equipped with hydraulically operated wedge grips. A surface mounted extensometer was used to measure axial strain for all conducted tests. A FLIR SC5000 Series IR camera was utilized to measure the variation of the test specimen surface temperature in situ and in real-time. The IR camera pixel resolution of 320×240 and temperature sensitivity of 20 mK was sufficient for accurately monitoring the temperature variation. The IR camera was synchronized to the test controller in order to trigger the acquisition of images at the same point in each loading cycle (i.e., at maximum stress), which was necessary to eliminate any variation in temperature due to reversible thermoelastic heating [13]. A photograph of the experimental setup employed for all tests is shown in Fig. 2.

There were two main types of tension-tension fatigue tests conducted in this study, both in accordance with test standard ASTM D3479 [23]. The first set of tests consisted of load-controlled fatigue tests subjected to a constant amplitude sinusoidal waveform with a loading frequency of 10 Hz and a stress ratio of 0.1. Various maximum stress amplitudes were chosen for different tests, where each test was conducted until failure or until a run-off of 10,000,000 cycles was reached in order to produce an $S-N$ curve. A minimum of three tests were conducted for each maximum applied stress. *Post mortem* sectioning of a number of these test specimens was also done in order to inspect for microscopic damage by scanning electron microscopy (SEM). The second set of tests consisted of the application of the thermographic approach for determining the HCFS of the PMC material. These tests were conducted in load-control, with a loading frequency of 10 Hz and a stress ratio of 0.1. The test specimen was subjected to a maximum stress amplitude for 7000 loading cycles, which was sufficient to produce temperature stabilization. The maximum stress amplitude was increased and the test specimen was subjected to another 7000 cycles; a number of stress levels were chosen and this process was repeated until the specimen failed. Note that only

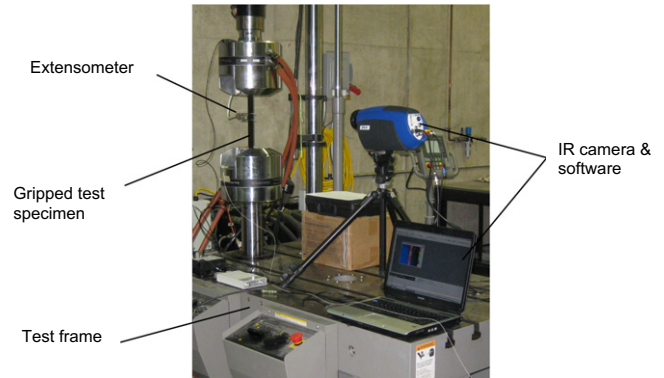


Fig. 2. Photograph of experimental setup using IR camera.

one test specimen was used to develop similar plots as shown in Fig. 1, which is another clear advantage of the thermographic approach for determining the HCFS. In total, three test specimens were used to conduct three sets of tests with the aforementioned procedure, which produced repeatable results.

5. Results and discussion

5.1. Development of $S-N$ curve with conventional approach

Static tests were initially conducted to determine the ultimate tensile strength (UTS) of the braided material [24], which was ultimately used to determine the maximum stress amplitude for the fatigue tests. A minimum of three test specimens were used for each maximum stress amplitude (50–85% UTS) to conduct the indicated fatigue tests. The fatigue life values corresponding to each test conducted at each maximum applied stress were used to create the $S-N$ curve shown in Fig. 3. The data point shown for a maximum stress of 100% UTS and 1 cycle to failure corresponds to the specimen static strength. The plot is linear on the log-scale from the static strength to the apparent HCFS, which was found to be in the range of approximately 60–65% UTS. For the test specimens cycled at maximum stresses below the HCFS, there was no failure after a run-off of 10,000,000 loading cycles. From many fatigue studies found in the literature it appears that conventional composite laminates do not typically have a fatigue limit, but instead damage progresses during the entire life of the material which causes failure even at lower applied stresses [25]. It should also be noted that most of these studies are discontinued prior to applying lower maximum stresses, causing an uncertainty of whether a true fatigue limit actually exists. It has been recently shown that some PMC materials do exhibit a fatigue limit or HCFS, which may be due to a damage saturation state at lower applied stresses hindering the onset of failure. This may not necessarily be a true fatigue limit but a new ‘finite life region’ for the material that is

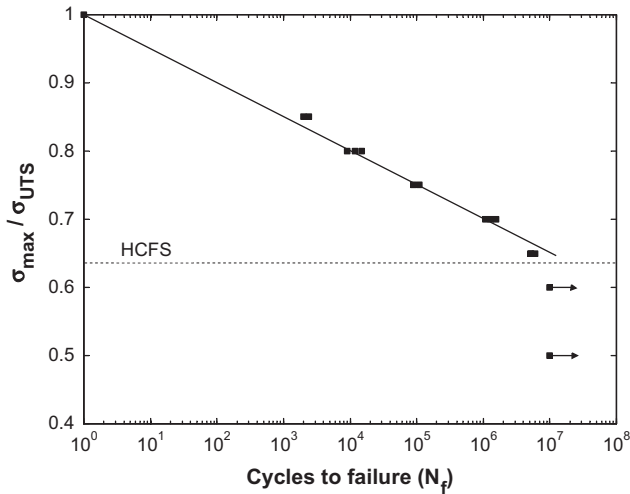


Fig. 3. Material S–N curve ($R = 0.1, f = 10$ Hz).

distinct from the main slope of the S–N curve as that shown in Fig. 3 [18].

Fig. 4 is a plot of the normalized stiffness degradation for 50%, 60%, 65%, 70% and 80% UTS test specimens. After 10,000 loading cycles, the 50% and 60% specimens exhibited a residual stiffness of approximately 94%, while the residual stiffness for the higher maximum stress amplitude specimens is below 92%. There is a clear gap in the stiffness profile between the lower and the higher maximum stress amplitude specimens, which further supports the discovery of a HCFS in the 60–65% UTS range. Various cross-sectional samples were obtained from a number of tested specimens for SEM observations; some test specimens were sectioned after fracture while others were sectioned prior to fracture. A series of photomicrographs obtained using SEM are shown in Fig. 5 for various test specimens. The main damage mode observed in all tested specimens was cracking in the $\pm\theta$ fiber yarns propagating along the yarn length, which was widespread throughout the width and length of all test specimens. For the test specimens cycled at 50–60% UTS, the majority of the $\pm\theta$ fiber yarn cracks arrested at the 0° fiber yarn interface without further propagation in the transverse direction. For the specimens cycled at 65–80% UTS, the $\pm\theta$ fiber yarn cracks developed into yarn interface cracks at the $0^\circ/\pm\theta$ fiber yarn

interfaces. In addition, cracking at the $+\theta/-\theta$ fiber yarn interfaces was found in the 65–80% UTS test specimens, along with significant cracking in the matrix-rich zones and through-the-yarn-thickness cracking in the 0° fiber yarns. From Fig. 5 it can be further deduced that the yarn interface cracks are generally wider and there is local matrix deformation for the specimens cycled at 65–80% UTS. The additional damage modes for the specimens cycled at 65–80% UTS would explain the increase in the stiffness degradation for those test specimens, and would also cause the additional energy dissipation providing further support for the existence of a fatigue limit or HCFS.

5.2. Determining HCFS using thermography and energy dissipation

The results for rapidly determining the HCFS using the thermographic approach will now be presented. Fig. 6 is a plot of the surface temperature as a function of the number of loading cycles for a test specimen, which was obtained using the IR camera. The maximum stress magnitude is indicated for each profile in the plot. The same location was used for each stress level to create the temperature profiles shown in Fig. 6, which was at the eventual failure location of the test specimen. Fig. 7 shows a sequence of surface temperature profiles, after stabilization, for the indicated maximum applied stress levels. Up to a cyclic load of 55% UTS, there is uniform temperature across the specimen surface. As the load increases there is a clear region where the temperature is higher (i.e., a hot zone), which is where the specimen ultimately failed. The temperature profile reached a stabilized plateau for all indicated stress levels. Note that although the specimen failed during the 85% UTS segment prior to reaching 7000 loading cycles, the temperature stabilized over a short range of cycles prior to failure. Using each corresponding stabilization temperature, the temperature increase is plotted as a function of the maximum applied stress in Fig. 8. The maximum stress magnitude at which the dissipated heat increase is greater is clear in the plot, which shows the characteristic bilinear profile. This corresponds to an approximate HCFS of 64% UTS, which is within the range obtained using the conventional S–N curve approach previously presented. This demonstrates that the rapid determination of the HCFS for this braided PMC material has been accurately obtained with the thermographic approach.

The accuracy of the thermographic technique necessitates further investigation into why this approach is successful for this

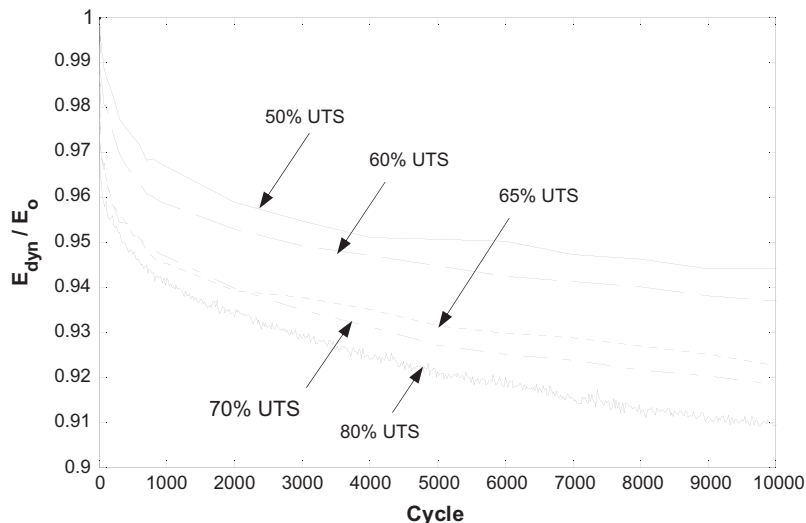


Fig. 4. Normalized stiffness degradation.

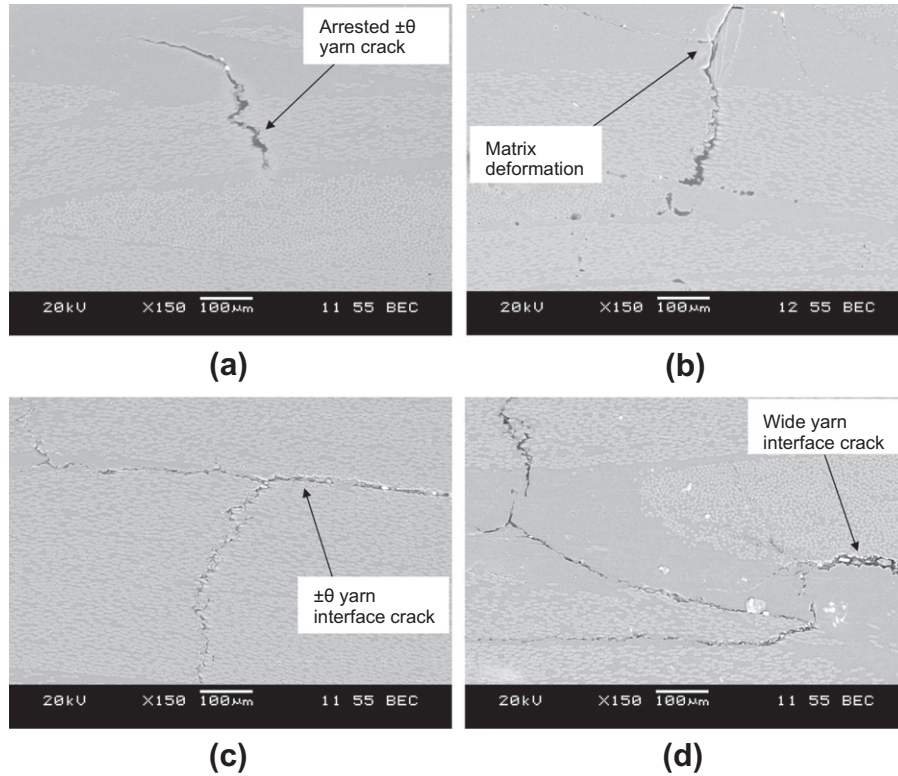


Fig. 5. SEM photomicrographs of (a) 50% UTS $\pm\theta$ yarn crack, (b) 70% UTS $\pm\theta$ yarn and matrix cracks, (c) 70% UTS $\pm\theta$ yarn interface crack, and (d) 80% UTS wide matrix/interface cracking.

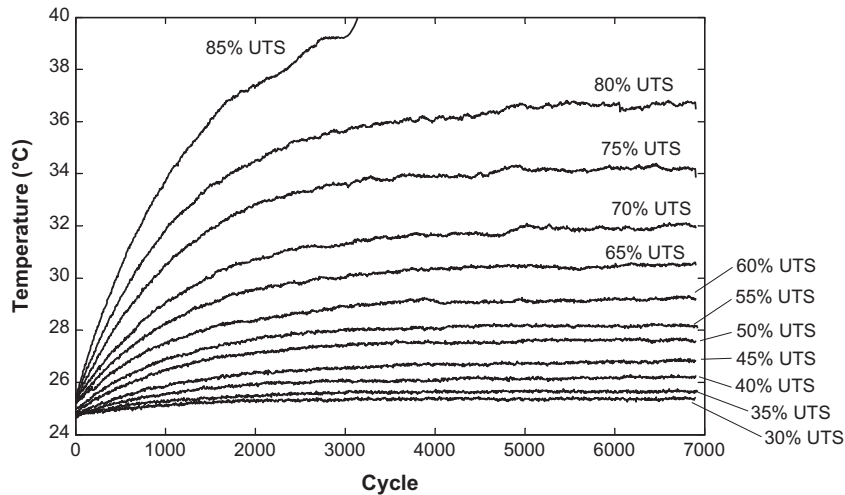


Fig. 6. Temperature profile vs. cycle for indicated maximum stress magnitudes.

textile PMC material. Recall that intrinsic energy dissipation in composites during fatigue, which may be caused by cracking or local matrix deformation, results in heat dissipation every cycle. If the energy dissipated per cycle is considered, a correlation between the temperature rise and the energy dissipation can in fact be made. The energy dissipated per unit volume of material during one loading cycle (i.e., hysteresis) can be determined by quantifying the area within the fatigue cycle stress–strain curve as shown schematically in Fig. 9. Although it may be difficult to directly calculate the energy dissipated on a cycle-by-cycle basis from experimental data, storing a sufficient number of data points per cycle during testing can yield fairly accurate predictions [26]. In this

study, 80 data points were found to be sufficiently accurate for calculating the dissipated energy per cycle. This was done by numerically integrating the stress–strain data cycle-by-cycle to obtain the area between the curves. The calculated dissipated energy per unit volume (E_d) was governed by the following equation (see Fig. 9).

$$E_d = \int_{\epsilon_{\min}}^{\epsilon_{\max}} \sigma_{\text{load}}(\epsilon) d\epsilon - \int_{\epsilon_{\min}}^{\epsilon_{\max}} \sigma_{\text{unload}}(\epsilon) d\epsilon \quad (3)$$

The equation assumes that smooth continuous functions for stress–strain exist, which was the case for the textile PMC material. These functions for the loading and unloading data points were

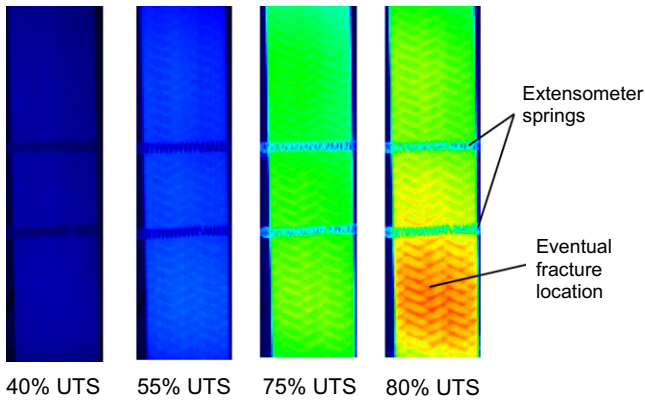


Fig. 7. IR temperature distribution after stabilization, center portion of test specimen.

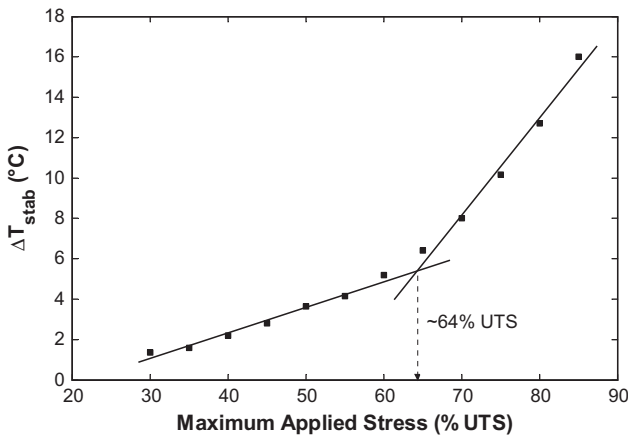


Fig. 8. Increase in temperature to stabilization vs. maximum stress magnitude.

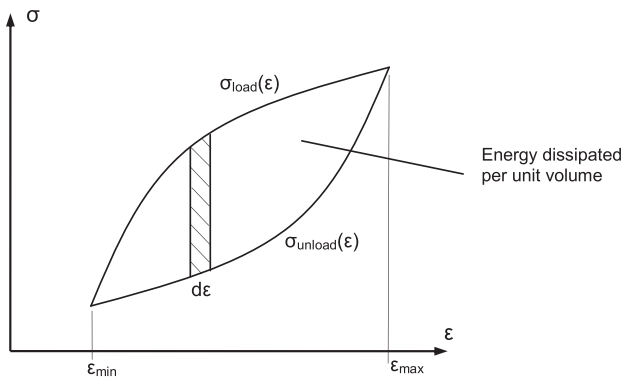


Fig. 9. Schematic for quantifying energy dissipation per unit volume per cycle.

determined through a regression analysis. By comparing the energy dissipated during a particular cycle in the fatigue tests during which temperature is stable (e.g., cycle 5000 or cycle 5500) for each maximum applied stress, a correlation between the energy dissipation and the maximum applied stress was established. A plot of the energy dissipated per unit volume (for cycle 5000) as a function of the maximum applied stress is shown in Fig. 10a. A similar bilinear profile was obtained using the energy dissipation as the HCFS indicator. A HCFS value of 63% UTS was found for the composite material, which is similar to that obtained using the thermographic approach (compare Figs. 8 and 10a). A plot of

the increase in temperature at stabilization vs. the energy dissipation per unit volume is shown in Fig. 10b. The relation between the temperature rise and the energy dissipated per cycle is in fact linear, as is shown in Fig. 10b with an R^2 data correlation value close to 1. This supports the hypothesis that the dissipated heat measured with the IR camera during cycling is in fact due to the intrinsic energy dissipation of the material, which is another important finding in this study.

5.3. Determining entire S–N curve using thermography

A HCFS was successfully established for the triaxially braided PMC material, which itself provides useful information for the design of structural components manufactured from this material. The thermographic technique can also be utilized to determine the entire fatigue curve as was done by Risitano and co-workers for various metallic alloys [27]. In the study, a direct linear relationship was established between the stabilization temperature increase (ΔT_{stab}) and the number of cycles to failure (N_f) for each maximum stress magnitude. This resulted in the definition of an integration parameter (Φ), which was a function of the stabilization temperature and the number of cycles to failure and defined by $\Phi = \Delta T_{stab} N_f$. This parameter, which was directly proportional to heat dissipation, was found to be constant regardless of the applied maximum stress magnitude. Thus, knowing this parameter one could determine the number of cycles to failure at any applied stress level higher than the fatigue limit. The direct application of this method did not yield similar results in the current study since a linear relationship between ΔT_{stab} and N_f was not established with the presented thermographic data, resulting in an inconsistent integration parameter. A different relationship between ΔT_{stab} and N_f was however determined. The stabilization temperature was found to be directly proportional to $\log N_f$, which yielded a constant integration parameter based on the definition in the following equation:

$$\Phi = \Delta T_{stab} \log N_f = \text{constant} \quad (4)$$

The assumption that for the majority of the life of each test specimen the measured surface temperature is constant (i.e., in the stabilization region on the temperature-cycle curve as in Fig. 1a) was also assumed in this study. This assumption ensures the integration parameter defined in Eq. (4) is accurate, since Φ is in effect the area under the ΔT – N curve [27], or in this study the ΔT – $\log N$ curve. The dissimilarity in the relationship between the stabilization temperature and the number of cycles to failure (when compared to the mentioned study on metallic alloys) may in fact be a characteristic of PMC materials. This can be manifested by the variation in the slope of typical S–N curves for PMC materials when compared to S–N curves of typical metallic alloys. In fact, a similar analysis on a different advanced material may produce a different relationship between ΔT_{stab} and N_f , which may result in another distinct definition of the integration parameter Φ . This is however beyond the scope of this study.

The average value for the integration parameter for the braided PMC material was approximately $\Phi_{avg} = 51.8 \text{ } ^\circ\text{C} \log(\text{cycle})$, with a standard deviation of $\pm 5.0\%$. Using the average integration parameter and the corresponding stabilization temperatures found using the IR camera, the number of cycles to failure for various maximum stress magnitudes were calculated and included on the S–N curve as asterisks shown in Fig. 11. The previously obtained HCFS is also included in the plot. An excellent agreement with the experimental data was obtained providing support for the rapid thermographic approach to determine the entire S–N curve for PMC materials, which is a key finding of this study. With this particular PMC material, as with metallic alloys, a direct relationship between the quantity of dissipated heat over the life of a test specimen and the number of cycles to failure was established.

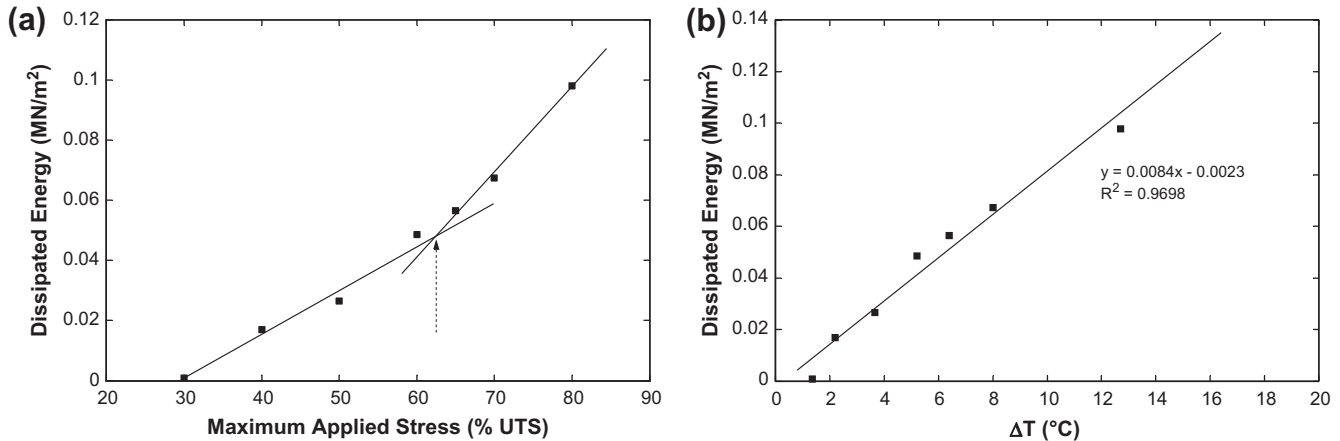


Fig. 10. Dissipated energy per unit volume during cycle 5000 vs. (a) maximum applied stress, (b) increase in temperature at stabilization.

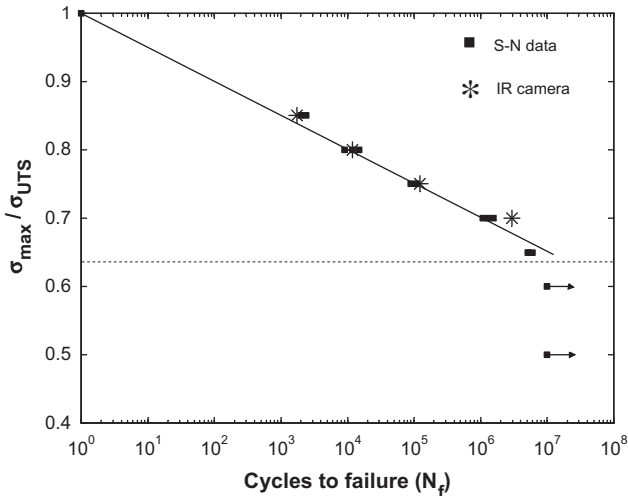


Fig. 11. Material S–N curve with calculated values of N_f shown as asterisks.

6. Conclusions

A variation of the thermographic approach for rapidly determining the fatigue behavior was employed and tested for a triaxially braided polymer composite plate using an infrared camera. The high cycle fatigue strength determined using the thermographic approach showed excellent correlation with that established while developing the conventional stress-life curve. The characteristic fatigue behavior of this particular composite was demonstrated through stiffness degradation profiles and scanning electron microscopic images of damage, which clearly indicate the existence of a fatigue threshold. The main damage mechanisms responsible for the increase in heat dissipation, and ultimately fatigue failure were identified. The energy dissipated per cycle during fatigue loading was also used as an indicator to determine the fatigue threshold, providing an excellent correlation with both the thermographic and the conventional approaches. The energy dissipation was directly correlated to the temperature rise during cycling, which supports the hypothesis that the dissipated heat measured with the infrared camera during cycling is in fact due to the intrinsic energy dissipation of the material. In addition, the thermographic technique was employed to rapidly determine the entire stress-life curve for the textile polymer composite materials. The results again provided an excellent correlation with the

conventional approach, which is a key finding in this study. It is further postulated that the definition of the integration parameter, which is vital for determining the entire S–N curve, may be distinct for other advanced materials. This was in fact the case in the present study, which is another useful finding for future application of this non-destructive technique. A direct correlation between the dissipated heat (measured as temperature), the intrinsic energy dissipation and the number of cycles to failure was established. Although additional experiments must be conducted to verify the usefulness of these methods for application to other composite materials, the presented results provide support for the rapid thermographic approach and reveal its effectiveness in assessing the fatigue properties of composite components. This study presented a novel application of the previously established rapid thermographic technique to determine the fatigue threshold and the entire S–N curve of a braided carbon fiber reinforced polymeric composite material, which is a significant contribution.

Acknowledgements

The authors would like to acknowledge the financial support of the Natural Sciences and Engineering Research Council (NSERC) of Canada. The financial support of the Canada Foundation for Innovation (CFI) and the Ontario Innovation Trust (OIT) towards the experimental research facility is also gratefully acknowledged. The first author also acknowledges additional funding in the form of a scholarship by NSERC.

References

- [1] Mouritz AP, Bannister MK, Falzon PJ, Leong KH. Review of applications for advanced three-dimensional fibre textile composites. *Composites Part A* 1999;30:1445–61.
- [2] Bannister MK. Development and application of advanced textile composites. *Proc Inst Mech Eng Part L – J Mater Des Appl* 2004;218:253–60.
- [3] Masters JE, Ifju PG. A phenomenological study of triaxially braided textile composites loaded in tension. *Compos Sci Technol* 1996;56:347–58.
- [4] Nakai A, Ohki T, Takeda N, Hamada H. Mechanical properties and microfracture behaviours of flat braided composites with a circular hole. *Compos Struct* 2001;52:315–22.
- [5] Tang G, Yan Y, Chen X, Zhang J, Xu B, Feng Z. Dynamic damage and fracture mechanism of three-dimensional braided carbon fiber/epoxy resin composites. *Mater Des* 2001;22:21–5.
- [6] Portanova MA. Tension and compression fatigue response of unnotched 3D braided composites. NASA Contractor, Report 1992, CR-189678.
- [7] Tate JS, Kelkar AD, Whitcomb JD. Effect of braid angle on fatigue performance of biaxial braided composites. *Int J Fatigue* 2006;28:1239–47.
- [8] Tate JS, Kelkar AD. Stiffness degradation model for biaxial braided composites under fatigue loading. *Composites Part B* 2008;39:548–55.
- [9] Bathias C, Cagnasso A. Application of X-ray tomography to the non-destructive testing of high-performance polymer composites. In: Masters JE, editor. *Damage*

- detection in composite materials – ASTM STP 1128. Philadelphia: ASTM International. p. 35–54.
- [10] Chen AS, Almond DP, Harris B. Acoustography as a means of monitoring damage in composites during static or fatigue loading. *Meas Sci Technol* 2001;12:151–6.
- [11] Bourchak M, Farrow IR, Bond IP, Rowland CW, Menan F. Acoustic emission energy as a fatigue damage parameter for CFRP composites. *Int J Fatigue* 2007;29:457–70.
- [12] Steinberger R, Valadas-Leitao TI, Ladstatter E, Pinter G, Billinger W, Lang RW. Infrared thermographic techniques for non-destructive damage characterization of carbon fibre reinforced polymers during tensile fatigue testing. *Int J Fatigue* 2006;28:1340–7.
- [13] Toubal L, Karama M, Lorrain B. Damage evolution and infrared thermography in woven composite laminates under fatigue loading. *Int J Fatigue* 2006;28:1867–72.
- [14] LaRosa G, Risitano A. Thermographic methodology for rapid determination of the fatigue limit of materials and mechanical components. *Int J Fatigue* 2000;22:65–73.
- [15] Luong MP. Fatigue limit evaluation of metals using an infrared thermographic technique. *Mech Mater* 1998;28:155–63.
- [16] Krapez JC, Pacou D. Thermography detection of damage initiation during fatigue tests. SPIE Conference – thermosense XXIV, Orlando, US, 1–4 April 2002, vol. 4710, p. 435–449.
- [17] Quaresimin M. Fatigue of woven composite laminates under tensile and compressive loading. ECCM-10, Brugge, Belgium, 3–7 June 2002.
- [18] Colombo C, Libonati F, Pezzani F, Salerno A, Vergani L. Fatigue behaviour of a GFRP laminate by thermographic measurements. *Eng Procedia* 2011;10:3518–27.
- [19] Colombo C, Vergani L, Burman M. Static and fatigue characterization of new basalt fibre reinforced composites. *Compos Struct* 2012;94:1165–74.
- [20] Chrysochoos A, Louche H. An infrared image processing to analyse the calorific effects accompanying strain localization. *Int J Eng Sci* 2000;38:1759–88.
- [21] Selezneva M, Montesano J, Fawaz Z, Behdinin K, Poon C. Microscale experimental investigation of failure mechanisms in off-axis woven laminates at elevated temperatures. *Composites Part A* 2011;42:1756–63.
- [22] Bremond P. Lock-in thermography: a tool to measure stress and to detect defects in aircraft industry. Canberra, Australia: AIAC; March 2001. 5–8.
- [23] ASTM, D 3479/D 3479M–96. Standard test method for tension–tension fatigue of polymer matrix composite materials. ASTM, International, 2007.
- [24] Montesano J, Fawaz Z, Poon C, Behdinin K. Characterization of the mechanical properties and fatigue behaviour of a three-dimensional braided carbon-fiber/polyimide composite. 2nd Joint US-Canada conference on composites, Montreal, September 26–28, 2011.
- [25] Harris B. A historical review of the fatigue behaviour of fibre-reinforced plastics. In: Harris B, editor. *Fatigue in composites - science and technology of the fatigue response of fibre-reinforced plastics*. Cambridge: Woodhead Publishing Ltd.; 2003. p. 3–35.
- [26] Giancane S, Panella FW, Dattoma V. Characterization of fatigue damage in long fiber epoxy composite laminates. *Int J Fatigue* 2010;32:46–53.
- [27] Fargione G, Geraci A, LaRosa G, Risitano A. Rapid determination of the fatigue curve by the thermographic method. *Int J Fatigue* 2002;24:11–9.